Geochemical characterization of a marine sediment core from the Joides Basin, Ross Sea, Antarctica

Geochemical characterization of a marine sediment core from Terra Nova Bay, Ross Sea, Antarctica

F. Burgay[1,2]*, O. Abollino[3], S. Buoso[4], E. Costa[5], A. Giacomino[3], C. La Gioia[4], S. Fraterrigo Garofalo[6], G. Pecoraro[7], M. Malandrino[4]

[1] Institute of Polar Sciences – National Research Council – Via Torino 155, Venezia Mestre

[2] Ca' Foscari University of Venice – Department of Environmental Science, Informatics and Statistics – Via Torino 155, Venezia Mestre

[3] Department of Drug Science and Technology, University of Torino, Via Giuria 9, Torino, Italy

[4] Department of Chemistry, University of Torino, Via Giuria 5, Torino, Italy

[5] Department of Earth Sciences, University of Torino, Via Valperga Caluso 35, Torino, Italy

[6] Department of Applied Science and Technology, Polytechnic University of Turin, Corso Duca degli Abruzzi, 24, Torino, Italy

[7] Sea Marconi Technologies, Via Ungheria 20, Torino, Italy

* → Corresponding author francois.burgay@unive.it

Abstract

The chemical fractionation of ten metals (Al, Ti, Cr, Fe, Cd, Cu, Mn, Pb, Zn and Ni) is reported for a marine sediment collected offshore in the Terra Nova Bay, Ross Sea, Antarctica. To evaluate their mobility and availability, the BCR sequential extraction procedure was applied on 11 sections of the sediment. The analyses, performed both by ICP-OES and GF-AAS, highlighted that most of the elements were in the residual phase, showing a strong binding with the matrix and a low availability. The BCR sequential procedure allowed us to have an insight into the chemical properties of the sediment and provided useful information about the redox state of the sediment itself and important indication on the availability and partitioning of different metals. A chemometric treatment was

applied on the dataset and it showed a separation between the superficial and the lowest sections of the core, the first being more influenced by the presence of Mn and the second by an increase in Al, Ti, Fe, Cr and Pb concentrations.

Keywords: Antarctica, Ross Sea, marine sediment, sequential extraction procedure, sediment diagenesis

1. Introduction

The Southern Ocean is the fourth largest ocean of the world. From the biological point of view, it is a so-called High-Nutrient Low-Chlorophyll (HNLC) region. In other words, it is characterized by a high concentration of nutrients, such as nitrates and phosphates, but it shows a very low productivity (Martin and Fitzwater, 1988; Martin et al., 1990). The main reason, as highlighted by Martin in 1990, is that this environment is Fe-limited. Through artificial (Smetacek et al., 2012) and natural (Duprat et al., 2016) Fe fertilization, it has been shown that the productivity increased with a significant atmospheric CO_2 drawdown to the surface ocean. Considering that one of the main Fe source to the ocean is the Aeolian mineral dust (Jickells et al., 2005), during the coldest and dustiest glacial periods, the increase in Fe supply caused an enhancement of the marine productivity in the Subantarctic zone of the Southern Ocean (Martínez-Garcia et al., 2011) that likely contributed to part of the total 100 ppm decrease in atmospheric CO_2 from the interglacial periods (Lambert et al., 2015).

The Ross Sea, which is the southernmost sea on Earth, is comprised between Victoria Land and Marie Byrd Land. It shows high marine productivity that contributes to at least half the annual biological production of the entire Antarctic continental shelf (48 Tg C yr^{-1}) (Arrigo and Van Dijken, 2003). Nowadays, the primary production has a peak during the austral spring and, according to satellite observations, can rise up to 4 g C m^{-3} d^{-1} (Rhodes et al., 2009). The productivity in the Ross Sea has been associated to the availability of Fe and it was found that algal community growth can

be limited by iron deficiency in much of the Southern Ross Sea during summer, excluding the areas where punctual iron sources exist (Sedwick et al., 2000). Taking advantage of the general absence of pollution (Caroli et al., 2001), the Ross Sea is a privileged spot where performing biogeochemical studies. On this purpose, marine sediment cores represent a unique archive to reconstruct the past seawater composition. The low-sedimentation rate that characterizes the off-shore regions of polar oceans (centimetres per thousand years) provides low-resolution records that can cover up to the last millions of years of the Earth history (Martínez-Garcia et al., 2011). The knowledge of their composition and of the involved sedimentation processes (i.e. biogenic, lithogenic and chemical processes) can be extremely helpful to address several environmental and climatic questions. For instance, through the determination of trace metals, it is possible to gain insight into the geochemical and environmental processes that took place in the water column or into the diagenetic processes that took place in the sediments themselves (Froelich et al., 1979).

Depending on how chemicals are bounded and on any pH or redox potential changes, sea sediments can act not only as a sink, but also as a new sources of trace metals and pollutants (Ianni et al., 2010). Therefore, to assess the environmental quality of a sediment core and to evaluate the more available fractions, it is crucial to perform fractionation studies using sequential extraction procedures. These methods are based on the use of a series of reagents chosen to solubilise in sequence different fractions thought to be responsible for retaining the trace metals (Gleyzes et al., 2002). The outcomes of sequential extraction procedures must be interpreted with caution because the reagents are not very selective and metal re-adsorption and redistribution may take place after each step. Nevertheless, such procedures provide useful information on metal binding mode and the possible presence of anthropogenic contamination (Bacon and Davidson, 2008). One of the most widespread sequential extraction procedures is the Tessier protocol (Tessier et al., 1979), that partitions the elements into five operationally-defined geochemical fractions including: exchangeable fraction; carbonate-bound fraction (acid-soluble); bound to Fe and Mn oxides fraction (reducible); bound to the organic matter fraction (oxidable) and residual fraction. However, considering the

diversity of existing procedures and the lack of uniformity among the different methods, a standardized three-step procedure was proposed by the former Community Bureau of Reference (BCR), now the Standards, Measurements and Testing Programme (Quevauviller, 1998). It involves three extractions steps with reagents of different strength in order to have information on the exchangeable, water- and acid-soluble (first step), reducible (second step) and oxidizable (third step) fractions. A comparison between the Tessier and the BCR protocol was performed on a Ross Sea sediment core. It highlighted higher extraction percentages for the Tessier procedure, mainly because of the stronger reagents and more drastic conditions (Casalino et al., 2013). In any case, considering the availability of a certified reference material, shorter extraction times, an easier sample handling and a detailed protocol, the adoption of the BCR procedure is preferable, especially if a comparison among different sites is subsequently performed. Nevertheless, the Tessier protocol can be advantageous when a distinction between a mobile and mobilizable fraction is object of studies (Casalino et al., 2013).

This paper reports the results of a geochemical investigation performed on one sediment core collected in Terra Nova Bay, Ross Sea, Antarctica, for ten metals: Al, Ti, Cr, Cd, Cu, Mn, Fe, Pb, Zn and Ni. We reconstructed both their total concentration and their partitioning in the different fractions according to the BCR procedure providing an insight on the diagenetic processes that might have taken place in the sediment itself. An X-Ray Diffraction (XRD) investigation to understand if the lithology of the sediment has changed over time is also reported.

2. Regional setting

The sediment core, coded sediment B, was sampled during the XX Italian Antarctic Survey in 2004-2005 at the mooring B (73°59.7’ S, 175°0.8’ E) in an offshore area of the Ross Sea. The collected sediment was located in the northern part of the Joides Basin at 588 meters depth (Figure 1). According to recent surveys performed at this location, the sinking particles are constituted mainly by lithogenic (40-62% of the composition of particles in the near-bottom trap) and biogenic materials

(29-47% of the bulk dry material in the near-bottom trap) (Langone et al., 2000). Their composition is strongly linked to the seasonal sea-ice cover: the lowest fluxes of biogenic silica were recorded during austral autumn and winter, when the sea-ice extent was at its maximum (Langone et al., 2000; Mezgec et al., 2017).

Ross Sea waters are generally oversaturated with respect to both calcite and aragonite, showing a saturation state greater than 1 (Hauck et al., 2012; Rivaro et al., 2014). The occurence of calcium carbonate species was well documented both in bottom traps (Bergami et al., 2009; Langone et al., 2000) and in deep sediment cores (Casalino et al., 2013). However, the high productivity of the Ross Sea and the respiration of the organic matter in the sediments can alter the sediment carbonate chemistry, modifying their preservation (Hauck et al., 2012). The mean $CaCO_3$ content in the Ross sea is 2% (714 g $CaCO_3$ m^{-2}) with the highest values (> 10%) being located in the Drygalsky Basin (Domack et al., 1999).

Sediment B features were investigated in previous studies (Ravaioli et al., 1999) where it was classified as siliceous mud. In particular, sediment B is constituted by olive-gray siliceous mud and ooze without gravels. The sediment is characterized by a high concentration of biogenic silica (20 to 30% of the total sediment mass). The concentration of organic carbon, ranging from 0.86 to 1.23%, does not show any clear trend along the core and it is the highest among all the investigated sediment cores in the Ross Sea (Frignani et al., 2003; Langone et al., 2000; Ravaioli et al., 1999). Compared to other sediment cores collected in different areas of the Ross Sea, sediment B is the one that shows the highest concentration of macrobenthos species, especially polychaetes (up to the 75%). These species, mainly located (80%) in the first 5 centimetres of the sediment, can provide potential bioturbation of the sediment itself (Ravaioli et al., 1999).

The Ross Sea topography is shaped by glacial erosion and it is characterised by a complex and heterogeneous morphology. This, results in a high variability in the sedimentation rates that can change up to two-orders of magnitude within a distance of less than 600 km (DeMaster et al., 1992).

In the Joides Basin, the ^{14}C sedimentation rate ranges from 4.5 cm kyr^{-1} to 42 cm kyr^{-1} (DeMaster et al., 1996; Langone et al., 1998; Mezgec et al., 2017; Salvi et al., 2004).

For sediment B, neither a ^{14}C dating nor a magnetic susceptibility profile were performed. For this reason, we compared the sediment accumulation rates (SAR) from different sediment cores collected close to sediment B (Figure 1; Table 1). Moreover, we observed that the diatomaceous mud layer, representative of Holocene open water conditions, has the same thickness both in site B and in site ANTA19-C14 (Corradi et al., 2003) which indicates similar sedimentation rates. In addition, site ANTA19-C14 has a ^{14}C sediment accumulation rate (38.3 cm kyr^{-1}) similar to the one calculated for sediment Y5 (38 cm kyr^{-1}), located less than 10 km away from site B. For these reasons, we assume that sediment B should preserve a SAR similar to the one calculated for the nearby sediments which ranges from 37 to 42 cm kyr^{-1}.

In this paper, we performed a comparison with other sea sediment cores collected in the Terra Nova Bay, which were analysed using the BCR extraction procedure. These sediments, coded D and H, were collected in a polynya area and on the outer continental shelf respectively (Casalino et al., 2013; Malandrino et al., 2010). They are characterized by a lower biogenic silica concentration than sediment B (1-4.5% and 5-8% respectively) and with low sediment accumulation rates of 1.7 cm kyr^{-1} (Frignani et al., 2003). The organic content is higher in sediment H (≈ 0.3%) than in sediment D (≈ 0.15%), with an enrichment at surface in both sites.

3. Material and methods

3.1 Sample processing

A stainless-steel box corer was used to sample 50 cm of sediment. The core was extruded from the corer and subsampled in different sections using a knife with a Teflon blade (Table 2). To avoid contamination from any metallic part, only the inner part of the core was collected and transferred into polycarbonate Petri boxes, stored at -25 °C and shipped to the University of Turin

(Italy). Subsequently, all the sections were defrosted for 18 hours in previously cleaned polycarbonate boxes under a Class-100 laminar flow hood located in a Class-100.000 clean room. They were dried under a Class-100 laminar hood, homogenized at 320 rpm for 15' and then stored in polycarbonate boxes. To take into account the moisture content, a sub-sample of sediment was dried at 105°C until constant mass was attained. Moisture contents were used to calculate all sediment characteristics on a dry mass basis.

We performed a sequential extraction procedure following the three-step Modified BCR protocol (Rauret et al., 2000). We will refer to the three extracted phases as the labile, reducible and oxidizable fractions respectively. All the bottles and vessels used during this process were previously filled for 7 days with a 5% solution of 65% HNO_3 (Sigma Aldrich Merck, USA), then rinsed with Ultrapure Water (UPW) and filled until their use with a 2% solution of 37% HCl (Sigma Aldrich Merck, USA). All the acids were purified by sub-boiling distillation in a quartz still and UPW was used throughout.

The labile fraction was extracted adding 20 ml of 0.11 M acetic acid (ACS Reagent, Honeywell, USA) to 0.5 g of sample in a reaction vessel. The sample was shaken for 16h at room temperature. The supernatant was then filtered and collected in previously cleaned polyethylene bottles, acidified with 100 µl of 65% HNO_3 (Sigma Aldrich Merck, 65%) and made up to 50. The residue was then washed with 10 ml of UPW.

The reducible fraction was extracted adding to the washed solid residual, 20 ml of a 0.1 M hydroxylamine hydrochloride (ACS Reagent, Merck, DE) solution adjusted to pH 2. The sample was shaken for 16h at room temperature. The supernatant was then filtered and collected in previously cleaned polyethylene bottles, acidified with 100µl of 65% HNO_3 (Sigma Aldrich Merck, USA) made up to 50 ml. The residue was then washed with 10 ml of UPW.

The oxidizable fraction was extracted adding to the washed solid residual, 5 ml of 33% H_2O_2 (Extrapure, Honeywell, USA) at room temperature for 1h. The solution was occasionally shaken. Then, the uncovered reaction vessel was heated at 85°C using a water bath for 2h until the total volume was reduced to 2 ml. 5 ml of 33% H_2O_2 were further added and kept for 1h at 85°C. Then the vessel was uncovered again until the final volume of 0.5 ml was reached. At this point, 25 ml of 1 M ammonium acetate (trace metal basis, Sigma Aldrich Merck, USA) (adjusted to pH 2 with 65% HNO_3) were added and the covered vessel was shaken for 16h at room temperature. The supernatant was then filtered and collected in previously cleaned polyethylene bottles, acidified with 100µl of 65% HNO_3 (Sigma Aldrich Merck, USA) and made up to 50 ml.

To have information on the total metal concentrations, an acid digestion in a Milestone MLS-12000 MEGA Microwave was also performed. 100 mg of dried sample were treated with 5 ml of *aqua regia* and 2 ml of hydrofluoric acid (48%, ACS Reagent, Sigma Aldrich Merck, USA) in PTFE bombs. The applied digestion program was: 300s at 250 W, 300s at 400 W, 300s at 600 W, 300s at 250 W. A ventilation step of 25 minutes followed. 0.7 g of boric acid were added and the bombs were further heated for 300s at 250 W and cooled again with a ventilation step of 15 minutes. The final solution was filtered and made up to 50 ml with UPW.

All experiments were executed in triplicate and the same procedure was performed for the blanks.

3.2 Apparatus and reagents

All the extracts were analysed either by ICP-OES (Varian Liberty 100 Inductively Coupled Plasma-Optical Emission Spectrometer) equipped with a V-groove nebulizer or by GF-AAS (Perkin Elmer 5100 Graphite Furnace Atomic Absorption Spectrometer) equipped with a heated graphite atomizer and Zeeman-effect background correction, depending on the concentration of the analytes in the samples and on the Limit of Detection (LoD) and Limit of Quantification (LoQ) (Table S2).

LoD, LoQ and more details on the instruments used for the determination of the different species are reported in the following sections. Calibration curves were performed using the external standard calibration method for all the ten elements of interest. Standards were prepared from single element 1000 mg L^{-1} stock solutions (Merck Titrisol).

X-ray powder diffraction (XRD) data were collected on specimens hand ground with an agate mortar and mounted on a zero-background Si-monocrystal flat sample holder, using an automated PW3050/60 PANalytical X'Pert-PRO diffractometer in Bragg-Bretano geometry with Θ-Θ setup, ~~Real~~ Real-Time Multile Strip detector and Cu-Kα radiation. Data were analysed in the 3-70° 2Θ range with the Diffrac Plus (2005) software (EVA 11,00,3).

4. Results

4.1 Quality assurance

The measurement trueness was evaluated both for the total digestion and for the sequential extraction method. For the total digestion, the MURST-ISS-A1 (Antarctic sediment) reference material (Caroli et al., 1998) was analysed using three replicates, while for the BCR protocol the BCR-701 (Lake Sediment) reference material was analysed (Casalino et al., 2013) using three replicates for each step. Regarding the total digestion of the sediment core and focusing on five main elements, the average recovery was 86 ± 9% (Table 3). Relatively to the BCR sequential extraction protocol, we found average recoveries of~~:~~ 81 ± 23 % for the first step, 91 ± 15% for the second step and 79 ± 15% for the third one (Table 4). Overall, our results underestimated the real concentration of some elements, in particular Zn (51%) in the first fraction and Cd (52%) in the third one. The uncertainty associated to each concentration value is comparable to the ones found in other studies (Cuong and Obbard, 2006).

The Limit of Detection (LoD) and the Limit of Quantification (LoQ) were determined through the ICP-AES and GF-AAS analyses of the blanks (number of readings: 3). The returned average

values were then summed to three times (for the LoD) and ten times (for the LoQ) the standard deviation of the blank measurements. The results are summarized in Table S1.

4.2 Total metal concentration and sediment lithology

Total metal concentrations in the core sections are reported in Table 5. Al, Fe and Ti are the metals with the highest concentrations. This indicates that they are the main constituents of the sediment lithology. The variability of each element along the core, expressed as relative standard deviation (RSD%), did not exceed 15%, apart from Mn (47%) and Cd (60%). This suggests that the lithology of the sediment did not significantly change within the studied period. Additional clues come from the XRD analysis performed on selected samples (B01, B02, B12, B17, B22, B27, B32, B37, B42, B45), which does not highlight any modification in the sediment composition (Figure S1). The sediment is mainly constituted by quartz (SiO_2), plagioclase ($(Na,Ca)(Si,Al)_4O_8$), K-feldspar ($KAlSi_3O_8$), mica $(Ca,Na)(Al,Mg,Fe)_{2,3}(Si,Al)_4O_{10}(OH)_2$ and halite (NaCl).

To quantify the carbonate concentration in the sediment we applied the Loss of Ignition method, based on the combustion of 1 g of dried sediment at 950°C for 2 hours (Heiri et al., 2001). More details on the analytical procedure and on the results are reported in the Supplementary Material (Figure S5). The results show that the carbonate content of the sediment ranges from 2% to 5% of the total dried mass reflecting the average calcium carbonate concentration retrieved from 52 sediments collected in the Ross Sea (Hauck et al., 2012). In our record, we found a significantly amount of trace elements associated ~~to~~ with the first BCR fraction. This fraction, as we will discuss deeply in the following, extracts metals that can be associated with carbonates. For this reason, and according to former interpretations of similar extraction results (Casalino et al., 2013; Ianni et al., 2010; Malandrino et al 2010), we hypothesize the presence of carbonate minerals, such as otavite ($CdCO_3$), rhodochrosite ($MnCO_3$) and siderite ($FeCO_3$) in our sediment core. Nevertheless, to better assess their occurrence, more focused investigations need to be performed (e.g. through Scanning Electron Microscope analyses).

4.3 Metal partitioning

The results of the metal partitioning will be interpreted assuming the following features (Abollino et al., 2006; Reddy et al., 2001): a) the first fraction corresponds to loosely held metal ions, including the exchangeable and soluble forms, that can be readily extracted and are therefore potentially available for the biota. Metals associated with carbonates and easily soluble oxide/hydroxides in mildly acidic conditions are present in the first fraction as well; b) the second fraction is composed of additional metal oxides/hydroxides soluble at acidic pH and metals associated with Fe-Mn oxides; c) the third fraction comprises metal ions associated with easily oxidizable solids or compounds, including organic matter and sulphides.

Figures 2-4 summarize the distribution of the elements in the four fractions. All the concentration values for each fraction and section are reported in the Supplementary Material (Table S4, Table S5 and Table S6)

Iron, aluminium, titanium and chromium (Figure 2): these elements are mainly present in the residual phase (> 80%) as silicates. This is consistent with the inert feature of these metals. Fe, despite its biological relevance, is also a key constituent of sedimentary rocks and it is mainly present in the sediment in its insoluble form (Gleyzes et al., 2002).

Zinc and copper (Figure 3): they are mainly extracted in the residual phase (> 50%). However, they are also present in high concentration along the whole core in the second and third fraction. This trend suggests that these elements are scavenged by amorphous oxides (Casalino et al., 2013) and ca be associated with humic and fulvic acids (10% and 20% for Zn and Cu respectively) (Braguglia et al., 1995). Low extraction percentages (from 4 to 14% and from 2% to 4% for Zn and Cu respectively) are recorded in the first fraction.

Nickel (Figure 3): it is present in a significant amount into all the different fractions showing a heterogeneous behaviour.

Manganese (Figure 3): it shows a peculiar fractionation as a function of depth. In the upper sections it is mainly extracted in the first and second fractions probably as rhodochrosite ($MnCO_3$) and as oxide (33% and 34% respectively), while below 6.5 centimetres depth, it mainly occurs in the residual phase.

Cadmium and lead (Figure 4): cadmium is mainly present in the acid-soluble phase ranging from 0.03 to 0.262 mg kg^{-1} with maximum values between 20 and 30 cm depth. Acid-soluble Cd constituted up to the 70% of the total Cd present in the sediment, while the remaining part is associated to Fe-Mn oxides. Cd is not detected in the oxidizable fraction. Lead is mainly extracted in the second and third fraction showing an opposite trend between these two fractions. In particular, lead associated with Fe oxides become increasingly more relevant with depth (from 17% to 67%), while a significant drop is observed in the oxidizable Pb fraction from 6 cm downwards (from 40% to 10%).

5. Discussion

5.1 Discussion on the total metal concentration

To determine if any anthropogenic contamination or any extra source affects the chemical composition of the sediment, we calculated the enrichment factors (EF) using the upper crustal elemental abundances (Hans Wedepohl, 1995) such that $EF = ([x]/c)_{sample}/([x]/c)_{upper\ crust}$ where c is one of the conservative crustal elements (i.e. Ti for our aims) and x the element we wanted to investigate (Table S3). Values higher than 10 indicate potential additional sources (e.g. pollution). However, we did not appreciate any value greater than 10. This confirms that all the geochemical evaluations that follow, are related to natural processes only.

Mn is more concentrated in the first 2 centimetres of the sediment, while its concentration decreases below 3.5 centimetres to a lower and almost constant value. Comparing our results with other studies performed in other locations of the Ross Sea (Casalino et al., 2013; Malandrino et al.,

2010), we found that sediment B represents a *unicum* concerning the total Mn behaviour. Both in site H (Casalino et al., 2013) and in site D (Malandrino et al., 2010), the total Mn concentration was higher (average: 1000 mg kg^{-1} and 544 mg kg^{-1} respectively) and with a lower variability along the core (RSD: 8% and 15% respectively). We interpreted this difference between sediment B and sediment D and H, as a consequence of different diagenetic processes related to the different sediment redox conditions that will be discussed in the following.

In sediment B, the Cd concentration increases with depth from an average of 0.06 mg kg^{-1}, recorded in the first 3 cm, to a maximum of 0.4 mg kg^{-1} at 27 cm depth. The average concentration along the whole core is 0.2 mg kg^{-1}, similar to the one recorded in site H (Casalino et al., 2013), but lower than the one recorded in site D (Malandrino et al., 2010).

The lower crustal element (e.g. Al, Fe, Ti, Mn) concentration recorded at site B than at site D and H can be linked to the higher SAR that characterizes this site. Considering that, at site D the highest values for these elements are- recorded in the deepest parts of the sediment, we hypothesize that, accordingly to the available sediment accumulation rate and ^{14}C dating (Frignani et al., 2003; Malandrino et al., 2010), this part corresponds to colder and dustier periods (e.g. Antarctic Cold Reversal). Alternative explanations can rely on the higher exposure to continental weathering (e.g. due to the strong katabatic winds) or on the faster degradation of the biological component than the mineralogical one in the bottom part of the sediment (Malandrino et al., 2010). This hypothesis is consistent with the progressive decrease in the total organic carbon concentration recorded in this sediment as a function of depth (Frignani et al., 2003).

A Principal Component Analysis (PCA) and a Hierarchical Cluster Analysis (HCA) were performed on the total element content (Figure 5). The PCA shows a clear correlation among Al, Ti, Fe, Cr and Pb which constituted the lithological bulk of the sediment, while the HCA shows a separation among the samples as a function of depth: 1) B01 and B02 forms one distinct group, mainly influenced by the high concentration of Mn. According to ~~with~~ the presence of macrobenthos in the

upper sections of the core (Langone et al., 1998), ~~it is possible that the first centimetres ar~~the first centimetres may be affected also by bioturbation processes; 2) from B07 to B22; 3) the sections from B27 to B37 are mainly influenced by Cu, Cd, Zn and Ni; 4) B42 and B45 are characterized by an increase in crustal elements such as Al, Ti, Fe, Cr and Pb. Contrarily to what described for sediment D, in this context, we exclude that this increase in the crustal element concentration can be linked to an increase in the organic matter degradation. Indeed, the organic matter concentration appears to be constant throughout the entire sediment (Ravaioli et al., 1999). This increase can be likely associated to external inputs that are difficult to identify in the absence of an absolute dating of the core.

We compared the average total concentrations of the elements in sediment B with the ones retrieved from other sites in the Terra Nova Bay (Table 6). The higher concentrations of Al and Fe in site D than in site B and H suggest that site D is more exposed to continental weathering. Furthermore, site D shows higher Cd concentration than sediment H and B. However, how we will discuss in the metal partitioning section, this increase is likely due to a stronger terrigenous input that characterizes the polynya than the other two sites. Site H and Site B show similar trace metals concentration ranges, likely because they are both located offshore.

5.2 Discussion on the metal partitioning

The distribution of manganese in marine sediments provides useful information on the sediment oxidation potentials (Pedersen and Price, 1982). In some circumstances, the presence of Mn(II)-carbonate is also considered a proxy for short oxygenation events in regions where anoxic conditions prevail (Lenz et al., 2014). Under these conditions, Mn, present in its reduced and soluble form (Mn^{2+}), is leached from the sediment and enriched in the anoxic stratified bottom waters. In case of short-term oxygenation events, soluble Mn^{2+} can be oxidized back to Mn-oxide. When the anoxic conditions are restored, it is reduced back to Mn(II) and, thanks to the alkalinity increase promoted by sulphur reducing bacteria, it can precipitate as rhodochrosite. These events are clearly visible in the sediment core stratigraphies as thin rhodochrosite layers (Huckriede and Meischner, 1996).

Mn species are also involved in the diagenesis of marine organic matter together with nitrate, Fe, and sulphate. Under semi-anoxic conditions, the organic carbon is oxidized by Mn(IV), which releases soluble Mn^{2+} to the porewater. Mn^{2+} can diffuse upwards in layers where more oxic conditions prevail and it can accumulate as MnO_2 (Froelich et al., 1979). This process provides a mechanism for stripping manganese from the deepest and anoxic sections of the sediment, accumulating and redepositing Mn oxides at the sediment-water interphase.

The adoption of the BCR protocol allowed us to investigate both the acid-leachable phase of Mn, where it is likely present as rhodochrosite (I fraction), and the reducible fraction, where it is present as oxide (II fraction). Our record shows that manganese extracted in the first fraction exhibits a maximum at 1 cm depth (40% of the total Mn, which corresponds to 201 mg kg^{-1}) followed by a decrease to the 3% of the total Mn concentration (4.6 mg kg^{-1}) from 8 cm depth to the bottom (Figure 3, Table S4). Mn-oxide concentration decreases sharply from 35% of the total Mn concentration (193 mg kg^{-1}) at the surface, to 10% at 6 cm depth (21 mg kg^{-1}, Figure 3, Table S5). This is consistent with what postulated by Froelich et al., (1979), which described an enrichment of Mn species at the sediment-water interphase and a subsequent pauperization of Mn-oxides in the anoxic part of the sediment. Thus, the Mn-oxide enrichment recorded at the surface can be explained as the re-oxidation of Mn^{2+}, which has migrated upwards from the anoxic section of the sediment through the sediment porewaters (Froelich et al., 1979).

The presence of a high concentration of labile-Mn, together with the high concentration of Mn-oxides at the water-sediment interphase, suggests that part of the Mn-oxides can be reduced by the respiration of the organic matter. Alternatively, a fraction of the total Mn^{2+} that diffuses upwards can precipitate as rhodochrosite instead of being oxidized by the O_2 excess. Lastly, the role of bioturbation in influencing the distribution of the Mn solid phase cannot be excluded *a priori*, considering the presence of different ~~macroozobenthos~~ macrozoobenthos species localized in the first 5 cm of the core (Ravaioli et al., 1999).

The interpretation of the Mn species distribution is consistent with the behaviour of the Fe species. Indeed, Fe is involved in the respiration of the organic matter under stronger anaerobic conditions (Wersin et al., 1991). In sediment B, we observed that, in the uppermost 3.5 cm, Fe extracted in the II fraction, builds up the 10-12% (from 1500 to 2500 mg kg^{-1}) of the total Fe. Below this horizon, the concentration of Fe oxides decreased down to the 4% (≈740-1000 mg kg^{-1}) of the total Fe (Table S4, Figure 2). This suggests that Fe(III) has been dissolved into soluble Fe(II) species accordingly to a plausible increase in the sediment anoxicity with depth. This interpretation is endorsed by the increase in the oxidizable Fe fraction with depth. Contrarily to what observed for the Mn species, the recycling of Fe upwards is reduced because of its tendency to be more easily captured by sulphide to form FeS species (Calvert and Pedersen, 1996).

Taking advantage from the availability of other two sediment cores in the Ross Sea (sediment H and sediment D) on which a BCR extraction procedure was performed, we investigated the differences in their redox states (Casalino et al., 2013; Malandrino et al., 2010). Neither sediment H nor sediment D show a significant variability in the Mn-oxides fraction that ranges from 3-7% and 2-6% of the total Mn concentration respectively. However, in sediment H the concentration of Mn-oxides is one order of magnitude higher (554 ± 134 mg kg^{-1}, 70% of total Mn) than in sediment D (25 ± 6 mg kg^{-1}). This, together with the absence of any enrichment in labile Mn along the whole core, indicates an overall oxic condition at this location. To the contrary, an increase in labile-Mn, is observed in the uppermost 3 cm of sediment D (15-6% vs 1% at the bottom). This layer, in the absence of a Mn-oxide enrichment, might indicate anoxic conditions of the site D bottom waters.

Organic complexes dominate the total concentration of Fe, Zn and Cu in seawater (Morel and Price, 2003). This behaviour is reflected in sediment B, where these metals, and especially Zn and Cu, are extracted in significant concentrations in the third fraction. In particular, these species exhibit an enrichment at intermediate depths (20-25 cm) where their concentration in the oxidizable fraction rise up to the 11% (for Zn), 26% (Cu) and 5% (Fe). Even if for Fe, a significant contribution can

come from the FeS species formed as a consequence of the respiration of the organic matter under anaerobic conditions, Zn and Cu are strongly bound to the organic matter as shown in another study performed close to site B (Calace et al., 2005). This can reflect the high productivity in this area, which causes a greater amount of organic and biogenic remains to get buried (Ianni et al., 2010).

In seawater, Cd shows a nutrient-like behaviour. Moreover, having, in its hydrated form, a similar ionic radius to that of the Ca ion, it can be taken up through the Ca-ion pumps by several marine organisms (Merian et al., 2004). This~~,~~ can result in ~~an~~ enrichment in the biogenic calcareous debris (Ciaralli et al., 1998; Ianni et al., 2010).The PCA performed on the first fraction (Figure S2) showed that Cd influences mainly the bottom sections of the core.

Comparing sediment B with sediment D, we observed that sediment D has a significantly lower average concentration of Cd associated to the first fraction, with the average value of 5.4 ± 4.8 %, but a higher total Cd content (up to 1.17 mg kg^{-1}). Considering that site D is a coastal site, this higher content in total Cd concentration can derive from a stronger terrigenous input (Malandrino et al., 2010). The lower concentration obtained in the first fraction might indicate a lower uptake from the marine phytoplankton at this location. This is consistent with the higher productivity recorded in site B than in site D (Frignani et al., 2003; Langone et al., 2000), that might have led to different Cd biological uptakes.

Accordingly with previous studies, we found that Mn and, especially, Fe oxides are good Pb scavengers (Ianni et al., 2010) since the largest fraction of Pb is associated with the II fraction. This is true in particular below 3.5 cm depth, where its concentration increased up to the 68% of the total Pb. It is also well known that the organically complexed lead fraction in seawater can constitute a significant portion of the total Pb (Capodaglio et al., 1998). In sediment B, a high amount of Pb is extracted in the oxidizable fraction (25-40%) in the uppermost 3.5 cm of the sediment. Considering the redox state of the sediment discussed above, we assume that Pb is bound to the organic matter rather than present as PbS. The increase in this fraction can be explained by the low concentration of

other micronutrients, which might have led to an increase in the Pb organic complexation in the water column. However, below 3.5 cm depth, the oxidizable Pb fraction decreased down to 8-10% of the total Pb. This is mirrored by an increase in the Zn and Cu extracted in the third fraction, which suggests a~~n~~ higher affinity of these micronutrients to the organic matter and produces a decrease in the concentration of organically bounded Pb, in favour of an increase in Pb scavenged by Fe-oxides (II fraction).

6. Conclusions

In this study, we showed the geochemical features of a sediment core collected in the Terra Nova Bay (Antarctica). Through a mineralogical study, we evaluated the lithology of the sediment and we found that it was mainly constituted by felsic rocks and it did not significantly change along the whole core. Most of the elements were present in the residual phase, indicating a strong binding with the sediment matrix and ~~a~~ low availability.

The BCR protocol allowed us to investigate in details the geochemical properties of the sediment highlighting several sediment diagenetic processes due to the respiration of the organic matter. Furthermore, we were able to understand which elements were bounded to the organic matter and which was their behaviour accordingly with their abundance and availability in the water column. Lastly, we discussed the role of Cd, which was mainly extracted in the first fraction. Because of the high organic carbon flux recorded at sediment B, we propose that the observed enrichment in labile Cd was mainly due to a non-selective biological uptake.

7. Data availability

All data are available upon request to the authors

Aknowledgments

This work was financially supported by the Italian National Antarctica Research Program (PNRA). We are grateful to Dr. Leonardo Langone for the precious support in providing us data from the oceanographic campaigns performed in the Ross Sea.

Tables and figures

Table 1 – Locations and sediment accumulation rates for sediments collected in the same area of sediment B.

Core	Coordinates	Sediment Accumulation Rate	References
Site B *(red dot)*	73°59.7'S; 175°0.8' E	n.a.	*This work*
ANTA91-14 *(violet dot)*	73°52.4' S; 175°24.8' E	38.3 cm kyr^{-1}	(Frignani et al., 1998)
Y5 *(green dot)*	74°00.0' S; 174°44.0' E	38 cm kyr^{-1}	(Calace et al., 2004)
WRS_JB *(blue dot)*	73°49.0' S; 174°39.0' E	42 cm kyr^{-1}	(Mezgec et al., 2017)
Site D *(black dot)*	75°06.0' S; 164°13.0' E	1.7 cm kyr^{-1}	(Malandrino et al., 2010)
Site H *(yellow dot)*	75°56.0' S; 177°36.0' W	1.7 cm kyr^{-1}	(Casalino et al., 2013)

Table 2 – Sections of the sediment and associated depth

Section	Depth /cm
B01	0-0.5
B02	0.5-1
B07	3-3.5
B12	5.5-6
B17	8.0-8.5
B22	11-12
B27	16-17
B32	21-22
B37	26-27
B42	32-34
B45	38-40

Table 3 – Cu, Cr, Zn, Mn and Mn recovery from the standard reference material MURST-ISS-A1. All values are reported in mg kg^{-1}.

	Analysed CRM value	Certified CRM value	Recovery %
Cu	5.15 ± 0.09	5.79 ± 1.59	89 %
Cr	30.8 ± 0.8	42.1 ± 3.4	71%
Zn	45.5 ± 0.1	53.3 ± 2.7	85%
Mn	420 ± 12	446 ± 19	94%
Fe	2.25 ± 0.07	2.44 ± 0.07	92%

Table 4 – Results of analysis of standard reference material BCR-701 in comparison with certified values for the different step of the BCR Protocol. All values are reported in mg kg^{-1}.

	Analyzed CRM value	Certified CRM value	Recovery %
Step 1			
Cd	5.7 ± 0.6	7.3 ± 0.4	78%
Cr	2.16 ± 0.05	2.3 ± 0.2	94%
Cu	57.7 ± 0.3	49.3 ± 1.7	117%
Ni	12.4 ± 0.4	15.4 ± 0.9	81%
Pb	1.97 ± 0.08	3.2± 0.2	62%
Zn	104 ± 8	205 ± 6	51%
Step 2			
Cd	4.18 ± 0.02	3.8 ± 0.3	110%
Cr	41.3 ± 0.3	46 ± 2	90%
Cu	82 ± 1	124 ± 3	66%
Ni	25.6 ± 0.7	27 ± 1	95%
Pb	108.0 ± 0.1	126 ± 3	86%
Zn	112 ± 2	114 ± 5	98%
Step 3			
Cd	0.14 ± 0.03	0.27 ± 0.06	52%
Cr	121 ± 5	143 ± 7	85%
Cu	38 ± 2	55 ± 4	69%
Ni	14.0 ± 0.6	15.3 ± 0.9	92%
Pb	7.4 ± 0.3	9 ± 2	82%
Zn	42 ± 1	46 ± 4	91%

Depth /cm	Cr	Mn	Zn	Ti	Cu	Al	Fe	Cd	Pb	Ni
-0.5	39.3 ± 0.6	624 ± 5	94.1 ± 0.5	2560 ± 20	29.5 ± 0.5	37000 ± 4000	24000 ± 2000	0.10 ± 0.01	9.0 ± 0.3	19.9 ± 0.4
-1	39.5 ± 0.4	544 ± 9	89 ± 1	2560 ± 20	29.4 ± 0.3	34000 ± 3000	22000 ± 1000	0.06 ± 0.02	8.7 ± 0.4	18.4 ± 0.2
-3.5	40.7 ± 0.5	321 ± 7	89.8 ± 0.6	2680 ± 40	29.0 ± 0.9	33500 ± 100	23500 ± 200	0.04 ± 0.01	9.1 ± 0.4	16.8 ± 0.3
-6	40.6 ± 0.4	248 ± 6	88 ± 2	2570 ± 20	30 ± 1	36000 ± 2000	23000 ± 1000	0.12 ± 0.01	11.6 ± 0.3	17.1 ± 0.8
-8.5	42 ± 1	226 ± 4	87 ± 1	2600 ± 20	31.1 ± 0.5	35000 ± 2000	21000 ± 1000	0.24 ± 0.02	11.4 ± 0.3	22 ± 5
-11	39.3 ± 0.2	210 ± 4	82 ± 2	2500 ± 40	34.4 ± 0.9	37000 ± 6000	22000 ± 2000	0.25 ± 0.01	10.6 ± 0.5	18 ± 1
-17	38.5 ± 0.3	204 ± 3	94 ± 2	2420 ± 40	33.3 ± 0.9	33000 ± 2000	19600 ± 900	0.48 ± 0.02	7.7 ± 0.2	19.9 ± 0.1
-22	40.4 ± 0.5	210 ± 2	100.4 ± 0.2	2530 ± 50	35 ± 1	35000 ± 2000	22000 ± 2000	0.37 ± 0.01	8.4 ± 0.1	21.2 ± 0.3
-27	43 ± 1	237 ± 6	109 ± 3	2780 ± 90	31.3 ± 0.2	36000 ± 1000	24000 ± 1000	0.37 ± 0.01	10.2 ± 0.3	22.9 ± 0.6
-34	47.1 ± 0.6	274 ± 3	110 ± 2	3070 ± 60	27.4 ± 0.7	45000 ± 6000	28000 ± 3000	0.28 ± 0.02	11.2 ± 0.7	23.7 ± 0.6
-40	45 ± 3	270 ± 20	95 ± 8	3000 ± 200	24 ± 1	43000 ± 7000	25000 ± 4000	0.37 ± 0.04	12 ± 1	20 ± 2
AV	41.3	306.1	94.4	2651.8	30.4	36772	23100	0.2	10	19.9
MAX	47.1	623.7	110.1	3069.8	34.7	45000	28000	0.5	12.2	23.7
MIN	38.5	204.4	81.5	2420.0	24.2	33000	19600	0.04	7.7	16.8
DEV	6	47	10	8	10	10	10	60	15	12

Table 5 – Total metal content. All concentrations are expressed in mg/kg. AV = average concentration. MAX = maximum concentration. MIN = minimum concentration. DEV = standard deviation (%)

Table 6 - Concentration ranges found in the sediment H (Casalino et al., 2013), sediment D (Malandrino et al., 2010) and sediment B (this work). Values are in mg kg^{-1}.

Element	Site D	Site H	**Site B**
Al	42 700-62 340	35 310-53 040	**33 000-45 000**
Cd	0.49-1.17	0.23-0.86	**0.04-0.5**
Cr	12-63	33-51	**39-47**
Cu	21-116	32-66	**24-35**
Fe	18 960-41 120	19 043-33 475	**19 600-28 000**
Mn	425-714	849-1176	**204-624**
Ni	16-36	13-34	**17-24**
Pb	15-31	10-15	**8-12**
Ti	2 670-3440	1 858-3 327	**2 420-3 070**
Zn	75-109	74-114	**81.5-110**

Figure 1 – Map of the Ross Sea. The red circle represents the sediment B (this study). The other cores are also shown: Y5 (green dot), WRS-JB (blue dot) and ANTA91-14(violet dot) where used for a better evaluation of the sediment accumulation rate. Site D (black dot) and site H (yellow dot) where used to perform a comparison. *Credits:* Antarctic Mapping Tools for Matlab (Greene et al., 2017)

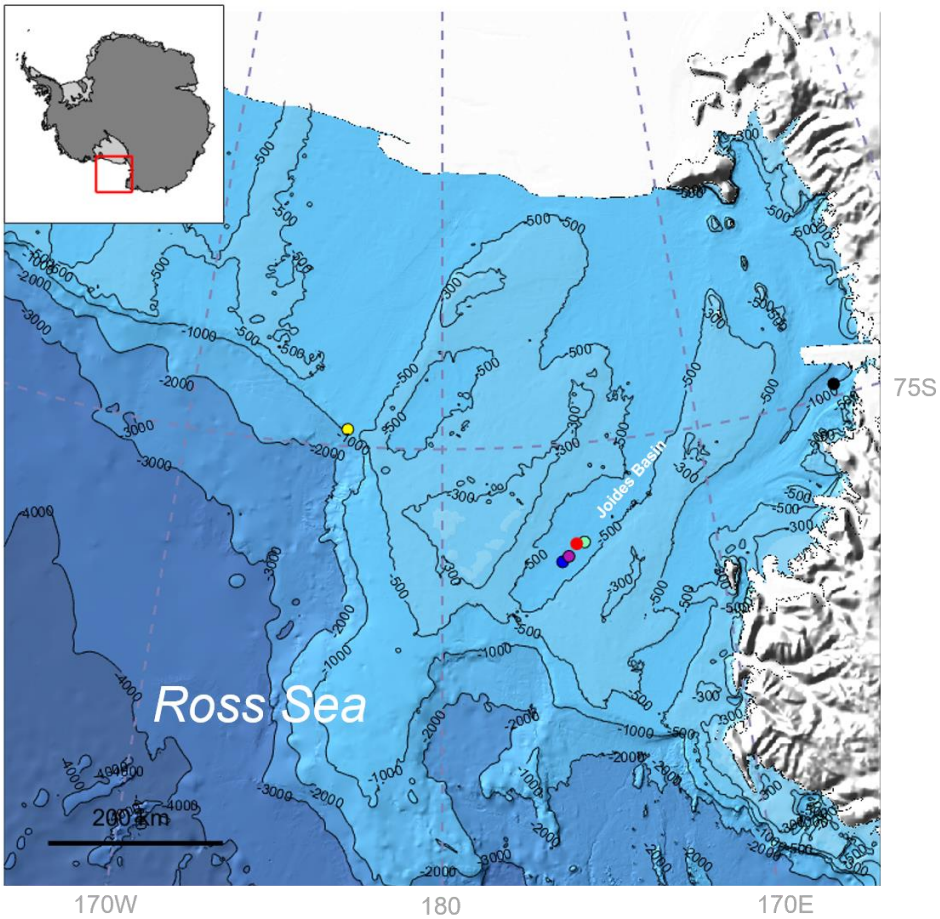

Figure 2 – Fe, Al, Ti and Cr partitioning among the BCR fractions: labile (Fraction I), reducible (Fraction II), oxidizable (Fraction III) and residual (total extracted minus the sum of the three fractions, Fraction IV).

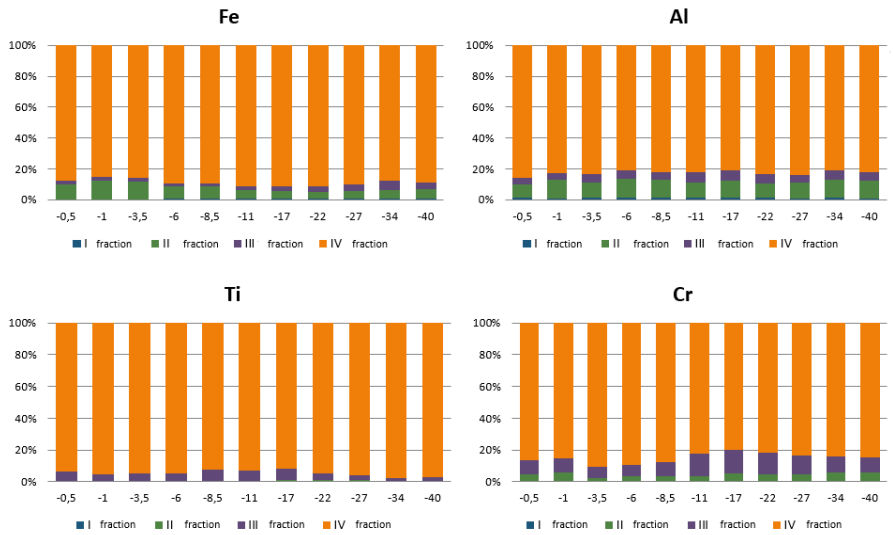

Figure 3 – Zn, Cu, Ni and Mn partitioning among the BCR fractions: labile (Fraction I), reducible (Fraction II), oxidizable (Fraction III) and residual (total extracted minus the sum of the three fractions, Fraction IV).

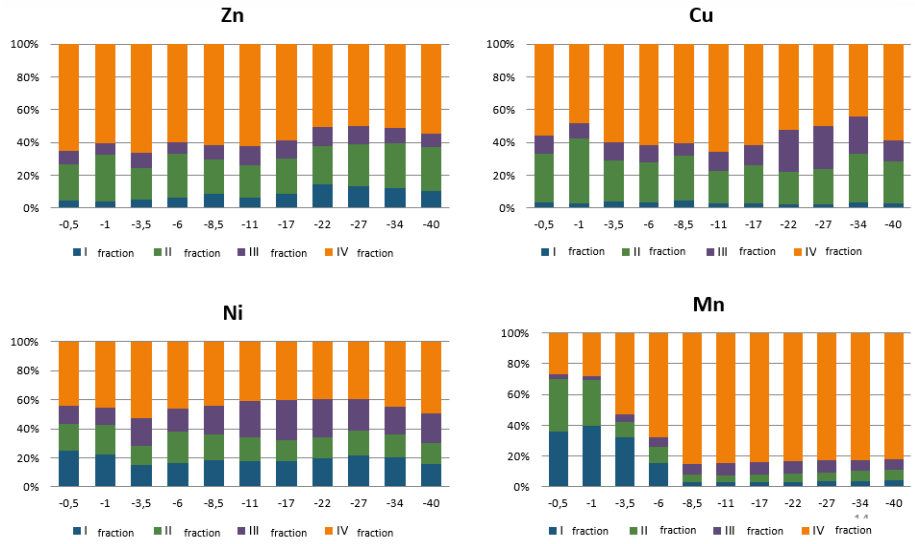

Figure 4 – Pb and Cd partitioning among the BCR fractions: labile (Fraction I), reducible (Fraction II), oxidizable (Fraction III) and residual (total extracted minus the sum of the three fractions, Fraction IV).

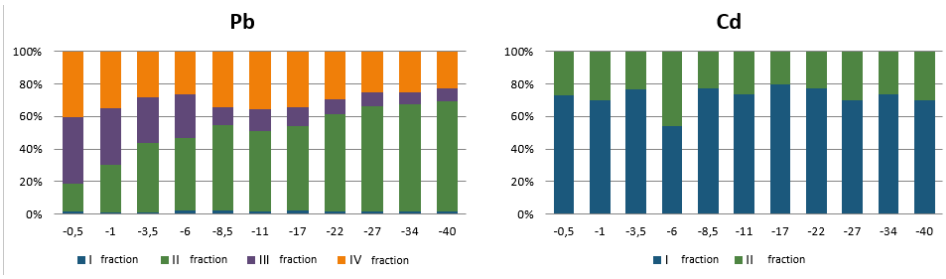

Figure 5 – Chemometric treatments on the total element content. *First panel*: bi-plot of scores and loadings on PC1-PC2; *Second panel*: dendrogram obtained by HCA.

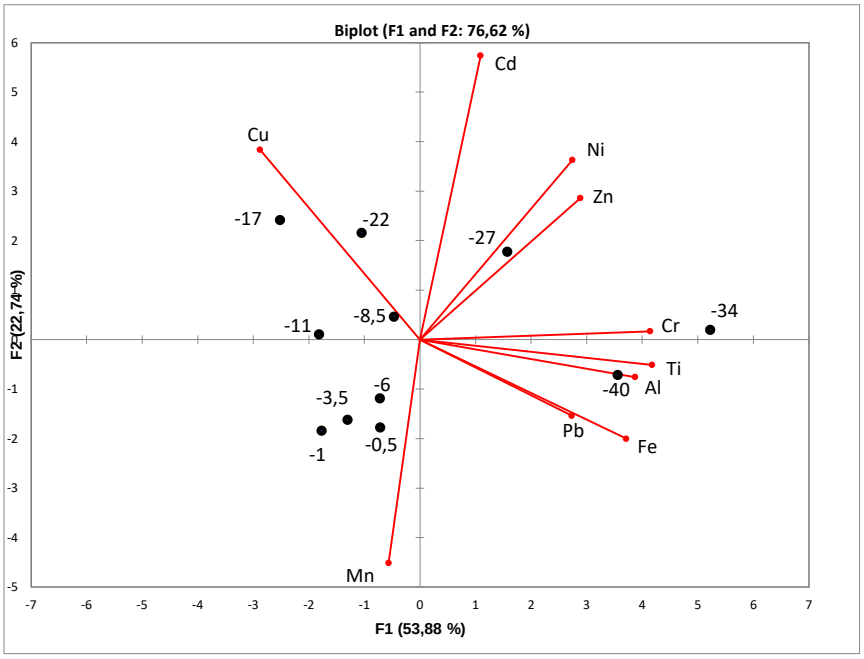

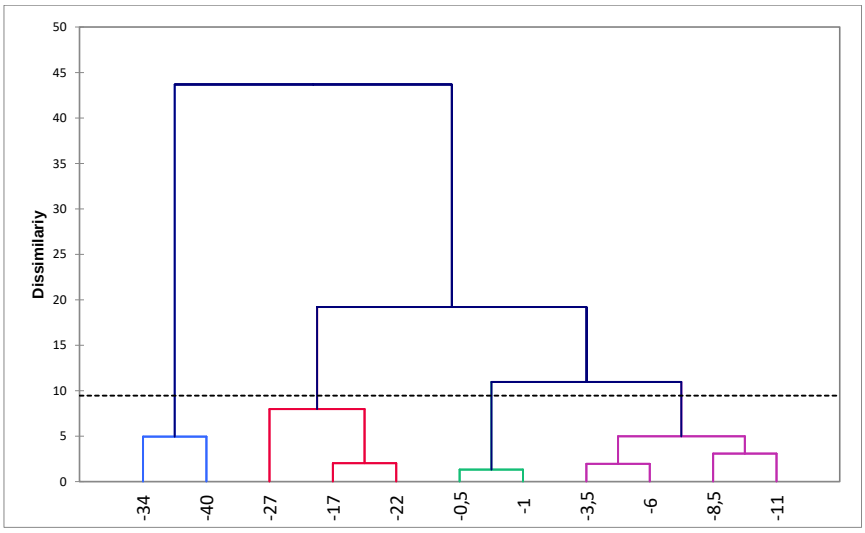

References

Abollino O, Giacomino A, Malandrino M, Mentasti E, Aceto M, Barberis R. Assessment of metal availability in a contaminated soil by sequential extraction. Water, Air, and Soil Pollution 2006; 173: 315-338.

Arrigo KR, Van Dijken GL. Phytoplankton dynamics within 37 Antarctic coastal polynya systems. Journal of Geophysical Research: Oceans 2003; 108.

Bacon JR, Davidson CM. Is there a future for sequential chemical extraction? Analyst 2008; 133: 25-46.

Bergami C, Capotondi L, Langone L, Giglio F, Ravaioli M. Distribution of living planktonic foraminifera in the Ross Sea and the Pacific sector of the Southern Ocean (Antarctica). Marine Micropaleontology 2009; 73: 37-48.

Braguglia C, Campanella L, Petronio B, Scerbo R. Sedimentary humic acids in the continental margin of the Ross Sea (Antarctica). International journal of environmental analytical chemistry 1995; 60: 61-70.

Calace N, Cremisini C, Galletti M, Mirante S, Petronio B. Copper and other trace elements strongly bound to humic acids along sediment cores in the Ross Sea, Antarctica. Journal of Environmental Monitoring 2005; 7: 1281-1286.

Calace N, Giglio F, Mirante S, Petronio BM, Ravaioli M. Sedimentary process inferences from humic substances analysis and deposition rates (Western Ross Sea, Antarctica). International Journal of Environmental Analytical Chemistry 2004; 84: 423-439.

Calvert S, Pedersen T. Sedimentary geochemistry of manganese; implications for the environment of formation of manganiferous black shales. Economic Geology 1996; 91: 36-47.

Capodaglio G, Turetta C, Toscano G, Gambaro A, Scarponi G, Cescon P. Cadmium, lead and copper complexation in antarctic coastal seawater. Evolution during the austral summer. International journal of environmental analytical chemistry 1998; 71: 195-226.

Caroli S, Cescon P, Walton DWH. Environmental contamination in Antarctica: a challenge to analytical chemistry: Gulf Professional Publishing, 2001.

Caroli S, Senofonte O, Caimi S, Robouch P, Pauwels J, Kramer G. Certified reference materials for research in Antarctica: the case of marine sediment. Microchemical journal 1998; 59: 136-143.

Casalino CE, Malandrino M, Giacomino A, Abollino O. Total and fractionation metal contents obtained with sequential extraction procedures in a sediment core from Terra Nova Bay, West Antarctica. Antarctic Science 2013; 25: 83-98.

Ciaralli L, Giordano R, Lombardi G, Beccaloni E, Sepe A, Costantini S. Antarctic marine sediments: distribution of elements and textural characters. Microchemical Journal 1998; 59: 77-88.

Corradi N, Fierro G, Giordano F, Ivaldi R, Langone L, Pitta A. High-resolution seismic mapping of the Holocene diatomaceous muddy drape in the Northern Joides Basin (Ross Sea, Antarctica). Terra Antartica Reports 2003; 9: 83-88.

Cuong DT, Obbard JP. Metal speciation in coastal marine sediments from Singapore using a modified BCR-sequential extraction procedure. Applied Geochemistry 2006; 21: 1335-1346.

DeMaster DJ, Dunbar RB, Gordon LI, Leventer AR, Morrison JM, Nelson DM, et al. Cycling and accumulation of biogenic silica and organic matter in high-latitude environments: the Ross Sea. Oceanography 1992; 5: 146-153.

DeMaster DJ, Ragueneau O, Nittrouer CA. Preservation efficiencies and accumulation rates for biogenic silica and organic C, N, and P in high-latitude sediments: The Ross Sea. Journal of Geophysical Research: Oceans 1996; 101: 18501-18518.

Domack EW, Taviani M, Rodriguez A. Recent sediment remolding on a deep shelf, Ross Sea: implications for radiocarbon dating of Antarctic marine sediments. Quaternary Science Reviews 1999; 18: 1445-1451.

Formattato: Italiano (Italia)

Duprat LP, Bigg GR, Wilton DJ. Enhanced Southern Ocean marine productivity due to fertilization by giant icebergs. Nature Geoscience 2016; 9: 219.

Frignani M, Giglio F, Accornero A, Langone L, Ravaioli M. Sediment characteristics at selected sites of the Ross Sea continental shelf: does the sedimentary record reflect water column fluxes? Antarctic Science 2003; 15: 133-139.

Frignani M, Giglio F, Langone L, Ravaioli M, Mangini A. Late Pleistocene-Holocene sedimentary fluxes of organic carbon and biogenic silica in the northwestern Ross Sea, Antarctica. Annals of Glaciology 1998; 27: 697-703.

Froelich PN, Klinkhammer G, Bender ML, Luedtke N, Heath GR, Cullen D, et al. Early oxidation of organic matter in pelagic sediments of the eastern equatorial Atlantic: suboxic diagenesis. Geochimica et cosmochimica acta 1979; 43: 1075-1090.

Gleyzes C, Tellier S, Astruc M. Fractionation studies of trace elements in contaminated soils and sediments: a review of sequential extraction procedures. TrAC Trends in Analytical Chemistry 2002; 21: 451-467.

Greene CA, Gwyther DE, Blankenship DD. Antarctic mapping tools for MATLAB. Computers & Geosciences 2017; 104: 151-157.

Hans Wedepohl K. The composition of the continental crust. Geochimica et Cosmochimica Acta 1995; 59: 1217-1232.

Hauck J, Gerdes D, Hillenbrand C-D, Hoppema M, Kuhn G, Nehrke G, et al. Distribution and mineralogy of carbonate sediments on Antarctic shelves. Journal of Marine Systems 2012; 90: 77-87.

Heiri O, Lotter AF, Lemcke G. Loss on ignition as a method for estimating organic and carbonate content in sediments: reproducibility and comparability of results. Journal of paleolimnology 2001; 25: 101-110.

Huckriede H, Meischner D. Origin and environment of manganese-rich sediments within black-shale basins. Geochimica et Cosmochimica Acta 1996; 60: 1399-1413.

Ianni C, Magi E, Soggia F, Rivaro P, Frache R. Trace metal speciation in coastal and off-shore sediments from Ross Sea (Antarctica). Microchemical Journal 2010; 96: 203-212.

Jickells T, An Z, Andersen KK, Baker A, Bergametti G, Brooks N, et al. Global iron connections between desert dust, ocean biogeochemistry, and climate. science 2005; 308: 67-71.

Lambert F, Tagliabue A, Shaffer G, Lamy F, Winckler G, Farias L, et al. Dust fluxes and iron fertilization in Holocene and Last Glacial Maximum climates. Geophysical Research Letters 2015; 42: 6014-6023.

Langone L, Frignani M, Labbrozzi L, Ravaioli M. Present-day biosiliceous sedimentation in the northwestern Ross Sea, Antarctica. Journal of Marine Systems 1998; 17: 459-470.

Langone L, Frignani M, Ravaioli M, Bianchi C. Particle fluxes and biogeochemical processes in an area influenced by seasonal retreat of the ice margin (northwestern Ross Sea, Antarctica). Journal of Marine Systems 2000; 27: 221-234.

Lenz C, Behrends T, Jilbert T, Silveira M, Slomp CP. Redox-dependent changes in manganese speciation in Baltic Sea sediments from the Holocene Thermal Maximum: An EXAFS, XANES and LA-ICP-MS study. Chemical Geology 2014; 370: 49-57.

Malandrino M, Mentasti E, Giacomino A, Abollino O, Dinelli E, Sandrini S, et al. Temporal variability and environmental availability of inorganic constituents in an Antarctic marine sediment core from a polynya area in the Ross Sea. Toxicological & Environmental Chemistry 2010; 92: 453-475.

Martin JH, Fitzwater SE. Iron deficiency limits phytoplankton growth in the north-east Pacific subarctic. Nature 1988; 331: 341.

Martin JH, Gordon RM, Fitzwater SE. Iron in Antarctic waters. Nature 1990; 345: 156.

Martínez-Garcia A, Rosell-Melé A, Jaccard SL, Geibert W, Sigman DM, Haug GH. Southern Ocean dust–climate coupling over the past four million years. Nature 2011; 476: 312.

Merian E, Anke M, Ihnat M, Stoeppler M. Elements and their compounds in the environment: occurrence, analysis and biological relevance: Wiley-VCH Verlag GmbH & Co. KGaA, 2004.

Mezgec K, Stenni B, Crosta X, Masson-Delmotte V, Baroni C, Braida M, et al. Holocene sea ice variability driven by wind and polynya efficiency in the Ross Sea. Nature communications 2017; 8: 1-12.

Morel FM, Price N. The biogeochemical cycles of trace metals in the oceans. Science 2003; 300: 944-947.

Pedersen T, Price N. The geochemistry of manganese carbonate in Panama Basin sediments. Geochimica et Cosmochimica Acta 1982; 46: 59-68.

Quevauviller P. Operationally defined extraction procedures for soil and sediment analysis I. Standardization. TrAC Trends in Analytical Chemistry 1998; 17: 289-298.

Rauret G, López-Sánchez J-F, Sahuquillo A, Barahona E, Lachica M, Ure AM, et al. Application of a modified BCR sequential extraction (three-step) procedure for the determination of extractable trace metal contents in a sewage sludge amended soil reference material (CRM 483), complemented by a three-year stability study of acetic acid and EDTA extractable metal content. Journal of Environmental Monitoring 2000; 2: 228-233.

Ravaioli M, Frignani M, Gambi M, Labbrozzi L, Langone L. Particle fluxes and sediment characteristics at three selected sites in the Ross Sea (Antarctica). Oceanography of the Ross Sea Antarctica. Springer, 1999, pp. 209-222.

Reddy KR, Xu CY, Chinthamreddy S. Assessment of electrokinetic removal of heavy metals from soils by sequential extraction analysis. Journal of hazardous materials 2001; 84: 279-296.

Rhodes RH, Bertler NA, Baker JA, Sneed SB, Oerter H, Arrigo KR. Sea ice variability and primary productivity in the Ross Sea, Antarctica, from methylsulphonate snow record. Geophysical Research Letters 2009; 36.

Rivaro P, Messa R, Ianni C, Magi E, Budillon G. Distribution of total alkalinity and pH in the Ross Sea (Antarctica) waters during austral summer 2008. Polar Research 2014; 33: 20403.

Salvi C, Salvi G, Stenni B, Brambati A. Palaeoproductivity in the Ross Sea, Antarctica, during the last 15 kyr BP and its link with ice-core temperature proxies. Annals of Glaciology 2004; 39: 445-451.

Sedwick PN, DiTullio GR, Mackey DJ. Iron and manganese in the Ross Sea, Antarctica: seasonal iron limitation in Antarctic shelf waters. Journal of Geophysical Research: Oceans 2000; 105: 11321-11336.

Smetacek V, Klaas C, Strass VH, Assmy P, Montresor M, Cisewski B, et al. Deep carbon export from a Southern Ocean iron-fertilized diatom bloom. Nature 2012; 487: 313-319.

Tessier A, Campbell PG, Bisson M. Sequential extraction procedure for the speciation of particulate trace metals. Analytical chemistry 1979; 51: 844-851.

Wersin P, Höhener P, Giovanoli R, Stumm W. Early diagenetic influences on iron transformations in a freshwater lake sediment. Chemical Geology 1991; 90: 233-252.